Energy Conversion and Management 75 (2013) 36–43

Contents lists available at SciVerse ScienceDirect

Energy Conversion and Management

journal homepage: www.elsevier.com/locate/enconman

Effect of flow rate, flow direction, and silica addition on the performance of membrane and the corrosion behavior of Pt–Ru/C catalyst in PEMFC

Farqad Saeed [a,*], Motasem Saidan [b], Adi Said [a], Mahmoud Mustafa [a], Amani Abdelhadi [a], Sarah Al-Weissi [a]

[a] Knowledge Sector, Royal Scientific Society, Amman, Jordan
[b] Chemical Engineering Department, University of Jordan, Amman, Jordan

ARTICLE INFO

Article history:
Received 15 February 2013
Accepted 24 May 2013

Keywords:
PEMFC
Flow rate
Pt–Ru/C catalyst
Nafion membrane

ABSTRACT

In order to evaluate the performance of Proton Exchange Membrane Fuel Cell (PEMFC) with an active area of 25 cm^2, several variables were studied (flow pattern, flow rate, degradation in the Pt–Ru/C catalyst). Polarization curves revealed that the electrochemical reaction on both sides of the fuel cell is under the effect of mass transfer and the values of the cell voltage, current density, and power density were inversely proportional with the increase of the hydrogen and oxygen flow rates for both flow patterns (counter current and cocurrent) and clear corrosion phenomenon was observed on the surface of the Pt–Ru/C catalyst before and after exposure to the hydrogen and oxygen. On the other hand and in order to increase the performance of Nafion membrane, SiO_2 particles were introduced to the Nafion polymeric matrix using sol–gel method to form composites. The surface morphology of the Nafion–SiO_2 composite membrane was investigated and compared with the existing commercial Nafion membrane. It was found that water uptake of the Nafion- silica composite membrane as a function of temperature is higher than that of the existing commercial Nafion membrane.

1. Introduction

In a typical PEM fuel cells, the membrane is sandwiched between two catalyzed electrodes to transport the protons, support the anode and cathode catalyst layers, and more importantly, separate the oxidizing (air) and reducing (hydrogen) environments on the cathode and anode sides, respectively. Therefore, the requirements for an excellent membrane are manifold and stringent, including high protonic conductivity, gas permeability, thermal and chemical stability, and so on. The most commonly used and promising membranes for PEM fuel cells are perfluorosulfonic acid (PFSA) membranes such as Nafion® (DupontTM). To prevent mechanical failure of the membrane, the Membrane Electrode Assembly (MEA) and flow field structure must be carefully designed to avoid local drying of the membrane, especially at the reactant inlet area. The membranes developed so far can be classified into three groups: (1) modified Nafion membranes, which are swelled with nonvolatile solvents or incorporate hydrophilic oxides and solid inorganic proton conductors; (2) alternative sulfonated polymers and their composite membranes, such as SPSF, SPEEK, PBI, and PVDF; and (3) acid–base polymer membranes, such as phosphoric acid-doped Nafion®–PBI composite membranes. With respect to the chemical and electrochemical degradation of the membrane, developing membranes that are chemically stable against peroxy radicals has drawn particular attention, Wu et al. [1].

Sridhar et al. [2], mentioned that low humidification greatly enhances membrane degradation during operation as well as under OCV. This behavior seems peculiar, because gas permeation through a Nafion membrane decreases with decreasing gas humidification. Basu [3], showed that Nafion membranes thickness ranges between (25 and 250 μm). Buchi [4], emphasized that corrosion of carbon supports may cause the electrical isolation and aggregation of platinum nanoparticles, causing a decrease in the ECA in the catalyst layers. Zhang [5], mentioned that the Gas Diffusion Layer (GDL) together with flow fields and current collectors, are designed to achieve high performance from the operation of the PEM fuel cell. Basu et al. [6], showed that Pt/Ru(40%:20% by wt.)/C and Pt-black could be used as a catalyst to prepare anode and cathode and carbon paper is used as substrate for the catalyst powder. Chul et al. [7], showed that Ti-felt with different structural properties (porosity and fiber diameter) and PTFE content were prepared for use as GDLs of the oxygen electrode, and the relation between the properties of the GDL and the fuel cell performance was examined for both fuel cell and electrolysis operation modes.

Hongtan and Andrew [8] showed that the difference in local electrical resistance under the land and channel is large enough to be a major cause for the observed local current density

* Corresponding author. Address: P.O. Box 1438, Al-Jubaiha 11941, Jordan. Tel.: +962 6 5344701x2707; fax: +962 6 5344706.
E-mail address: farqad.hadeethi@rss.jo (F. Saeed).

0196-8904/$ - see front matter © 2013 Elsevier Ltd. All rights reserved.
http://dx.doi.org/10.1016/j.enconman.2013.05.045

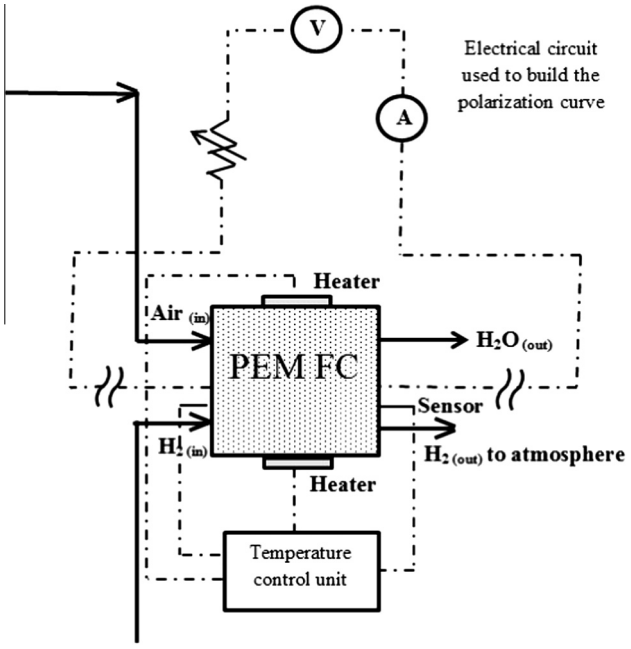

Fig. 1. PEM fuel cell setup.

differences. Kap-Seung et al. [9], studied the geometrical characterization of the serpentine flow-field in order to enhance the performance of PEMFC in relation to pressure drop, discharge of condensed water, maximization of cell voltage, and uniformity of current density over the entire surface area. Luis et al. [10], studied the influence of the relative entry positions of hydrogen and oxygen on the distribution of gases. Santarelli and Torchio [11] studied the effect of six operating conditions on the performance of single PEMFC: cell temperature; anode flow temperature in saturation and dry conditions; cathode flow temperature in saturation and dry conditions; and the reactants pressure while Hsieh et al. [12] studied the effect of cell temperature, gas humidification, cell operating pressure and reactant gas flow rate with interdigitated flow fields. On the other hand Miaomiao et al. [13], studied the water uptake and swelling ratio, thermal and chemical stability, mechanical properties, proton conductivity. Jin et al. [14] studied the polarization curves of a single PEMFC having a Nafion membrane fed with H_2/O_2 with relative humidity (RH) of 35%, 70% and 100% at cell temperatures ranging from 65 °C to 120 °C at back pressure of 0 atm and 1 atm, respectively. Afshari and Jazayeri [15] developed a fully numerical model of two dimensional, non-isothermal, electrochemical–transport to investigate simultaneous water, heat transport phenomena and their effects on PEM cell performance. Tian et al. [16] studied the carbon loading, PTFE content and species, sintering time, temperature and pore formers.

It is worth to mention that the current work is considered novel in comparison with the revised literature in terms of the studied parameters which play a vital role in the performance of the PEM fuel. In other words the work is based on studying the functionality of Nafion membrane and the corrosion behavior of the Pt–Ru/C catalyst due to hydrogen and oxygen as a function of the flow rates (5, 10 and 15 ml/min) and its directions (i.e. Counter and Cocurrent) in serpentine flow field at constant temperature (80 °C) in addition to studying the surface morphology and water uptake of the casted [Nafion, Nafion–SiO_2 composite] in comparison with the commercial membranes at various temperatures (i.e. 20, 35, 50, 65, 80 °C).

2. Experimental

2.1. Materials

The catalysts used to prepare the electrodes (cathode and anode) were Pt–Ru (40%, 20% by wt.)/C. Carbon black and carbon paper were used as a substrate for the mentioned catalyst. Nafion solution was used as a binder. Hydrogen with purity of 99.999% was used as a fuel. Air was supplied to the fuel cell as source of oxygen. Nafion dispersion was used to cast the proton exchange membrane in addition to commercial Nafion membranes. Sulphuric acid was used for activating both casted and commercial membranes. Isopropanol was used as diluent. Silicon dioxide was used to improve the water uptake of the casted Nafion membrane.

2.2. Membrane preparation

The Nafion [perfluorosulfonic acid]–SiO_2 membrane was casted from Nafion dispersion containing 4% wt. Nafion ionomer using sol–gel method, Alvarez et al. [17]. The isopropanol and Nafion dispersion were mixed in a 1:3 volume ratio, and then 1 mg of SiO_2 was added to selected samples. These samples were kept in an oven for 7 h at 100 °C until all solvent was evaporated and the polymeric ionomer forms a solid polymer membrane known as Nafion–SiO_2 composite membrane. Then the formulated membrane film was treated for 1 h in 1 M H_2SO_4 at 80 °C. Finally, it was rinsed in boiling distilled water for 1 h. The thickness of the resulted membrane was 103.2 μm.

2.3. Preparation of anode and cathode

Electrode of PEMFC should be porous to enable hydrogen and oxygen from air to diffuse through the anode and cathode active

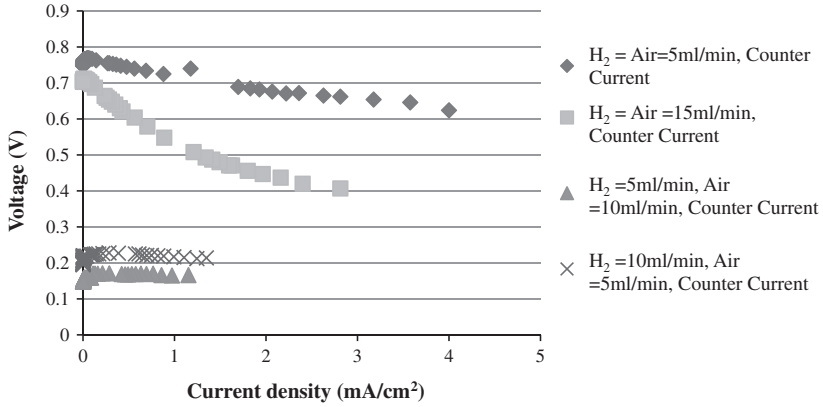

Fig. 2. PEMFC performance (operating conditions: counter current flow, 80 °C).

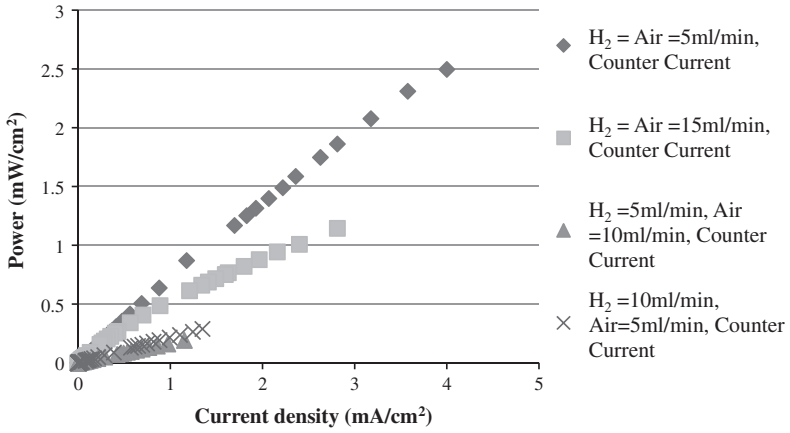

Fig. 3. PEMFC performance (operating conditions: counter current flow, 80 °C).

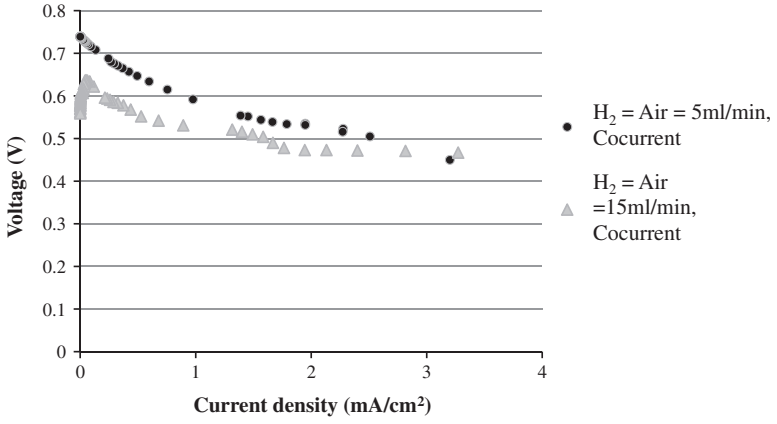

Fig. 4. PEMFC performance (operating conditions: cocurrent flow, 80 °C).

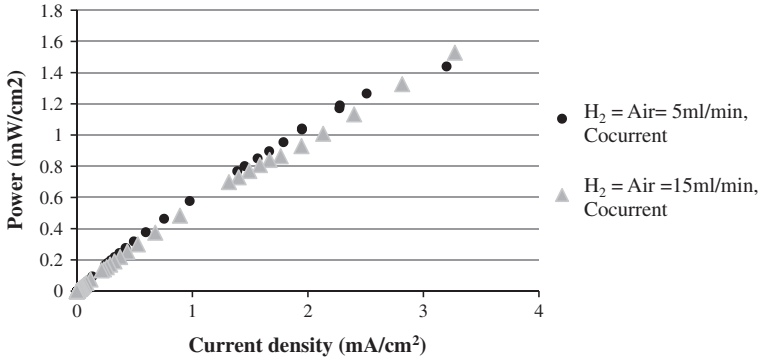

Fig. 5. PEMFC performance (operating conditions: cocurrent flow, 80 °C).

zone (Gas Diffusion Layer GDL) respectively. The anode and cathode were prepared by dispersing carbon black mixed with iso-propanol on the surface of 5 × 5 cm carbon paper, then left on-side the oven at 100 °C for 30 min in order to evaporate the iso-propanol. Slurry of Pt–Ru (40%–20% by wt.)/C, Nafion ionomer, PTFE, iso-propanol was spread over the carbon black layer in the form of continuous wet film using a brush, it was then dried in an oven for 30 min at 150 °C. Nafion ionomer acted as a binder while PTFE with pores at the cathode provided a network to expel water in order to minimize the occurrence of flooding.

2.4. PEM fuel cell experiments

PEM fuel cell tests were performed with a single cell of 25 cm^2 in area with serpentine flow fields. The MEA was fitted between two graphite unipolar plates with serpentine flow channels 1 × 1 mm for hydrogen and air flow. The cell was clamped between two gold plated plates using a set of retaining bolts positioned around the periphery of the cell. Electrical heaters with a control system were attached to each gold plated plate in order to heat the cell to the desired temperature. Hydrogen and air were fed

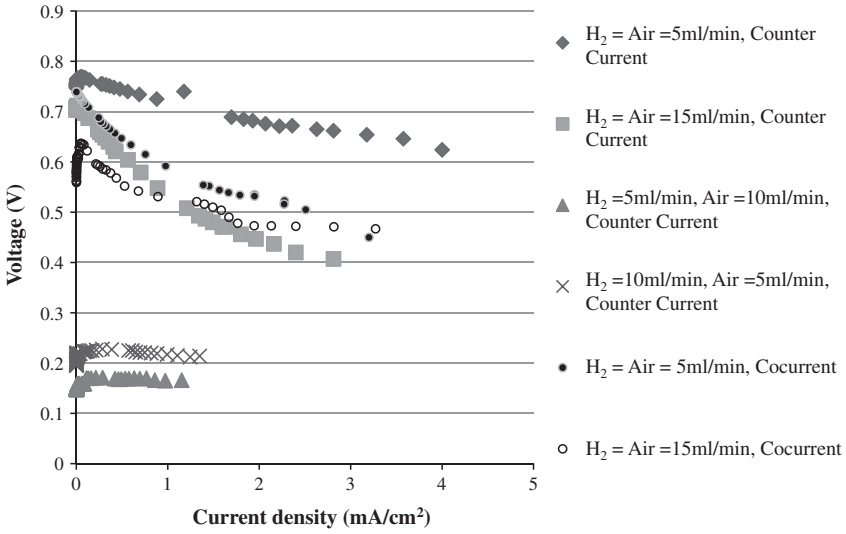

Fig. 6. PEMFC performance for counter and cocurrent flow at 80 °C.

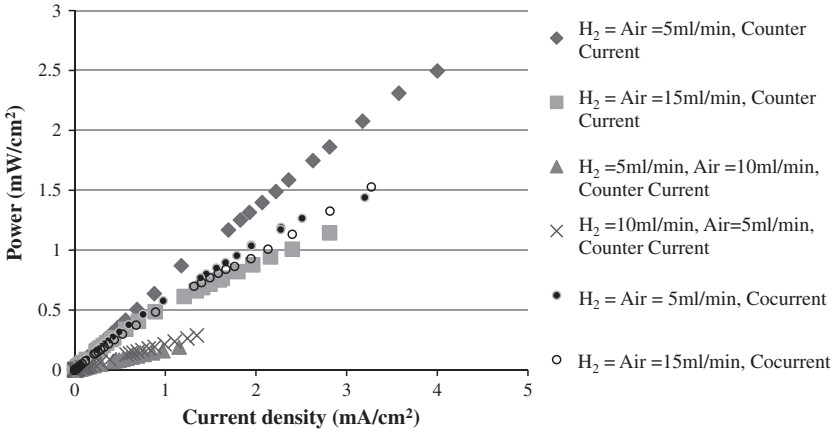

Fig. 7. PEMFC performance for counter and cocurrent flow at 80 °C.

Table 1
Chemical analysis of the gas diffusion layer and the catalyst layer before and after exposure to H_2 at the anode.

Elements	GDL + catalyst (before exposure to H_2) (%)	GDL + catalyst (after exposure to H_2) (%)
C	73.18	78.55
Ru	7.65	5.16
Pt	19.18	16.29
C	71.05	78.23
Ru	7.96	6.65
Pt	20.99	15.12

from two cylinders connected to the PEM fuel cell setup. Two flow meters with manual regulators were used to fix the flow at the desired value. Fig. 1 represents PEM fuel cell setup based on the above explanation.

2.5. PEM water uptake experiments

In order to investigate the water uptake of the Nafion–SiO_2 composite membrane in comparison with the commercial membrane, the following procedure was conducted:

(A) Keeping the various Nafion membranes (with SiO_2, without SiO_2, commercial) in the furnace for 8 h prior to each experiment at 100 °C to ensure its complete dryness from water molecules.
(B) Measuring the weight of the membrane before immersing in water.
(C) Immersing the membrane in a beaker containing distilled water at different temperatures (20, 35, 50, 65, 80) °C for 8 h for each temperature.
(D) Measuring the weight of the membrane after immersing in water (removing excess surface water), then the following relation was applied to calculate water content, Alvarez et al. [17]:

Table 2
Chemical analysis of the gas diffusion layer and the catalyst layer before and after exposure to air at the cathode.

Elements	GDL + catalyst (before exposure to air) (%)	GDL + catalyst (after exposure to air) (%)
C	73.18	78.53
Ru	7.65	6.99
Pt	19.18	14.48
C	71.05	77.29
Ru	7.96	6.48
Pt	20.99	16.23

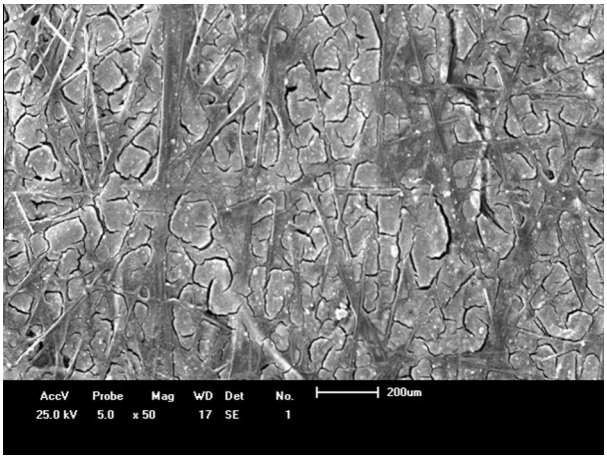

Fig. 8. Topography of catalyst layer before exposure to hydrogen and air.

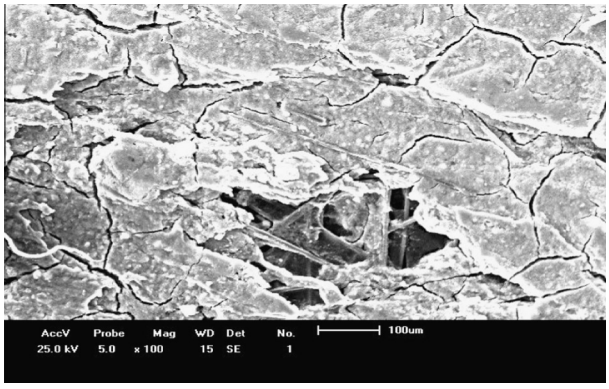

Fig. 9. Topography of catalyst layer after exposure to hydrogen gas. Obvious degradation in the layer was noticed.

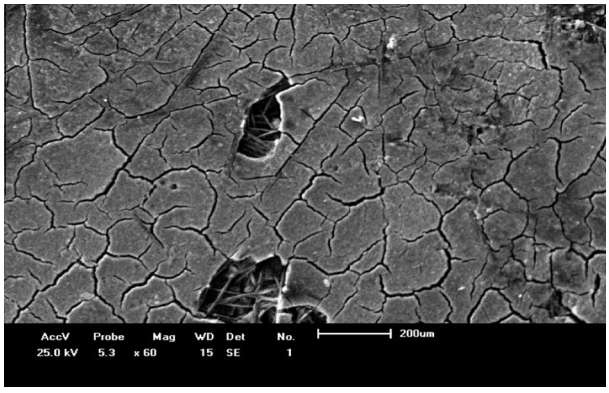

Fig. 10. Topography of catalyst layer after exposure to hydrogen gas. Obvious degradation in the layer was noticed.

$$\text{Water Content } (\%) = ((G_w - G_d)/G_d) * 100$$

(E) Plotting Water Content (%) vs. Temp. in (°C).

3. Results and discussion

3.1. Investigating the effect of flow pattern and the flow rate of hydrogen and oxygen on the performance of PEMFC

In order to identify the parameters that have direct influence on PEMFC performance, two flow patterns were selected (counter current and cocurrent) and various flow rates of hydrogen and air were investigated (5, 10, 15 ml/min) at 80 °C as shown in Figs. 2–7. The figures revealed that the cocurrent flow mode showed that the distribution of the current and power density decreases along the cell with increasing the flow rate. This decrease is mainly the derivative of the increase in the hydration of the membrane from the inlet to the outlet. This suggests at this cell voltage, the mass transport (mainly oxygen concentration) is the limiting step in the performance of the cell. As oxygen depletes across the cell, the current density decreases, while in the counter-flow configuration, the distribution of the current and power density along the cell followed the same trend of cocurrent flow but with higher values because of the combined effect of hydration of the membrane and the concentration of oxygen which was less in comparison with the cocurrent flow. On the other hand a sudden drop in the voltage indicates zero concentration of hydrogen on the catalyst surface. The current corresponding to this point of zero concentration of H_2 is called limiting current. A fuel cell cannot produce more than the limiting current because no reactants exist at the catalyst surface beyond this point on the *V–I* curve. In other words diffusion of ions have a great influence on the mass transport rate of reactants, Wang and Liu [18], Dietmar et al. [19] and Sreenivasulu et al. [20].

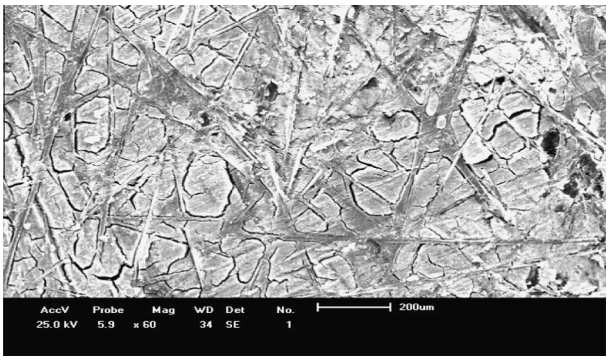

Fig. 11. Topography of catalyst layer after exposure to air. Obvious degradation in the layer was noticed.

3.2. Investigating the degradation in the catalyst and GDL

SEM and EDX analysis for the Gas Diffusion Layer (GDL) and the catalyst layer (i.e. Pt–Ru/C) revealed an obvious degradation in the elements of the layers before and after exposure to hydrogen (anodic side of PEMFC) and oxygen (cathodic side of PEMFC) as

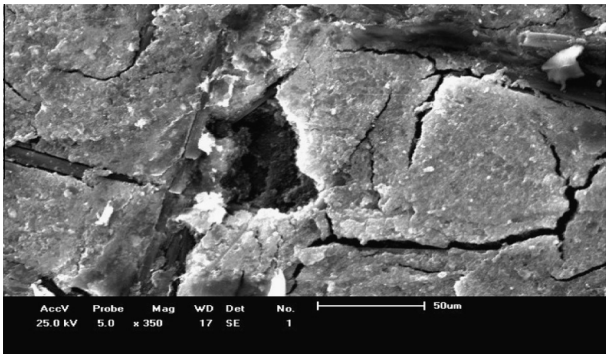

Fig. 12. Topography of catalyst layer after exposure to air. Obvious degradation in the layer was noticed.

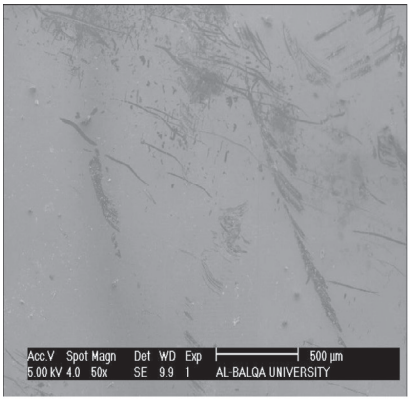

(a) Produced membrane in situ before adding SiO_2

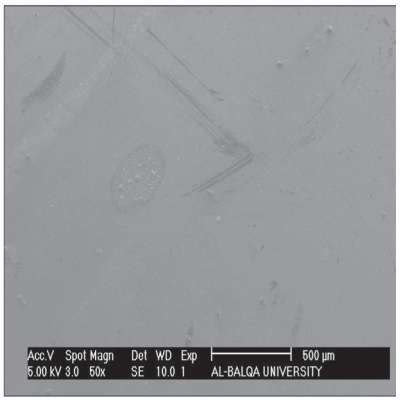

(b) EC-NM-115 Nafion membrane

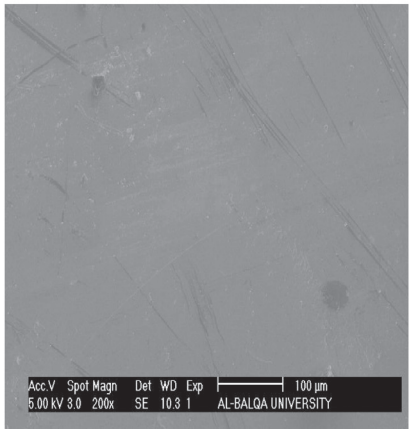

(c) EC-NM-117 Nafion membrane

Fig. 13. SEM images of different membranes.

shown in Tables 1 and 2 and Figs. 8–12 due to the corrosion phenomenon as a direct result of the electrochemical reaction between the catalyst layer in the anodic side and the hydrogen gas as well as the electrochemical reaction between the catalyst layer in the cathodic side and the water molecules formed due to the electrochemical reaction between H_2 and air, Park et al. [21]. It is obvious from Figs. 8–12, that the corrosion is affected by the flow of hydrogen and air. This emphasize the facts obtained from Figs. 2–7 which indicated that the electrochemical reaction is under the effect of mass transfer or concentration polarization following Eq. (1), Fontana and Greene [22], Uhlig [23], Revie [24], Bard and Faulkner [25] :

$$\eta = \pm\beta \log(1 - i/i_L) \tag{1}$$

where η is the overpotential, β is Tafel constant = 2.3 RT/$\propto$ $n{\cdot}F$. On the other hand i_L is the limiting diffusion current = $nFkC_b$, k is the mass transfer coefficient and C_b is the bulk concentration.

The galvanic coupling among dissimilar metals can be treated by application of mixed potential theory. Therefore, in the case of Pt–Ru (40%: 20% by wt.)/C three metals are connected to each other forming a galvanic active combination. The response of this combination to the corrosive environment (i.e. Hydrogen and Oxygen) differs from the behavior of these metals when they are not connected to each other, because each metal has its own exchange current density (i_o) and Equilibrium Potential (E_{eq}) and as a result the corrosion current (i_{corr}) will deviate in its position towards the coupling potential ($E_{coupling}$) rather than the corrosion potential of the metal when it is alone. As a result of this assumption the metals in the combination might show an increase in the current to less negative values and other might show a decrease in the current to less positive values. In other words, the behavior of these metals in the given environment might respond in different manners so the more negative (active) metal in the combination might corrode sacrificially and get depleted to protect the other metals of less negativity (i.e. more noble). This act is also affected with the surface area of each metal in the couple as an important variable. In our case Ru% is less than Pt% and C% and as a result there will be a difference in the area ratio of cathodic elements in the combination to anodic elements in same combination (Ac/Aa), raising the act of the sacrificial depletion of the most active metal in the combination to protect the other elements by generating tiny currents (negative and positive) so that the summation of the galvanic anodic currents generated by the three metals will be gathered by the most active metal in the combination while the summation of the galvanic cathodic currents will be gathered by the most noble metals in the combination. As a result galvanic corrosion will occur encouraging the formation of pitting corrosion as shown in the mentioned figures.

3.3. Characterizing and investigating the performance of the Nafion–SiO_2 composite membrane

The produced proton exchange membrane ‘‘Perfluorosulfonic acid membrane’’ (i.e. NAFION©) in situ by the mentioned method in the experimental section was transparent and with homogeneous phase distributions as compared to membranes which were commercially purchased. Fig. 13 shows scanning electron microscope (SEM) images for three different Nafion membranes

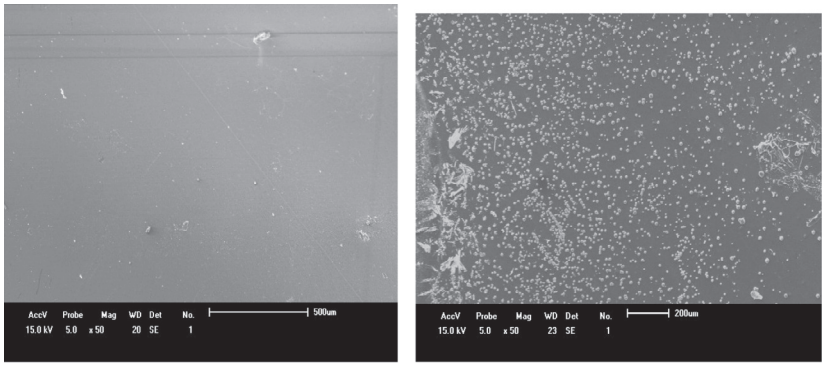

(a) Nafion membrane without SiO_2 (x50)

(b) Nafion membrane with SiO_2 (x50)

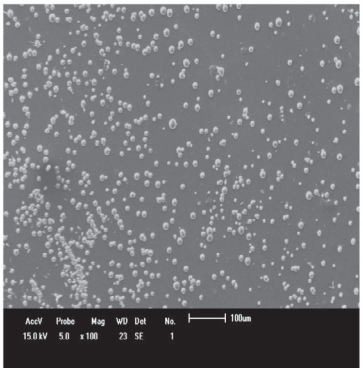

(c) Nafion membrane with SiO_2 (x100)

Fig. 14. SEM images of the produced membranes in situ with and without SiO_2.

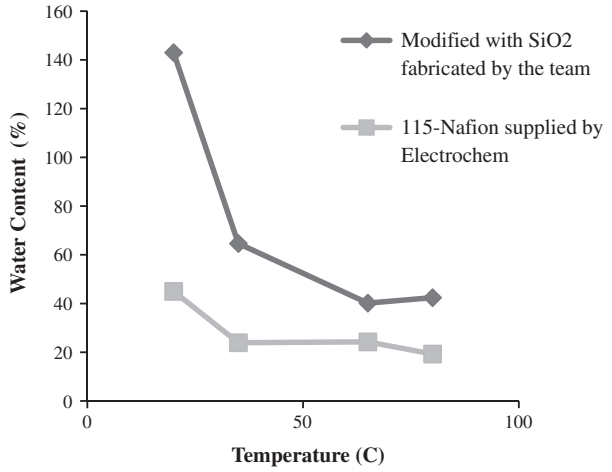

Fig. 15. Water uptake of the modified and commercial membrane.

prepared and purchased, demonstrating no phase separation. The SEM images shown in Fig. 13 shows that the Nafion morphology is reasonably consists a semi-crystalline regions within a continuous network. The semi-crystalline regions are hydrophobicregions made up of main chain tetrafluoroethylene segments; while the continuous network is hydrophilic regions consist of sulfonate groups Mauritz and Moore [26]. However, the spheres that are shown in Fig. 13 SEM images is supporting the model of Gierke et al. [27], known as the cluster-network model, which assumes that the sulfonate groups form into spherical clusters that resemble inverted micelles. The morphology have appeared in the three membranes, demonstrating morphological compatibility in the casted membrane. The SiO_2 particles have been impregnated in the membrane to form a Nafion–SiO_2 composite membrane as shown in Fig. 14. It is obvious from SEM images that the unagglomerated SiO_2 crystals (i.e. white particles) were uniformly distributed on the surface. The performance and hydrophilicity of the fabricated composite membrane have been investigated and compared to that for the commercial membrane (EC-N-115) at different temperatures. However, as it is shown in Fig. 15, the water uptake in the composite membrane is higher and better than that for the commercial membrane at different temperatures (i.e. 20, 35, 65, 80 °C) due to the existence of SiO_2 and because of the hygroscopic nature of metal oxides (SiO_2). The composite membrane water uptake depends on membrane hydration, however, the increased hydration improves membrane proton conductivity and fuel cell performance. Moreover, temperature and water content strongly affect Nafion's viscoelastic response, which are of direct importance for operating PEMFC. Accordingly, it is expected that the composite membrane has higher performance than the commercial Nafion membranes.

4. Conclusion

The results revealed that type of flow pattern (counter or cocurrent), flow rate (i.e. hydrogen and oxygen on both sides of the fuel cell (anode and cathode) play an important role in the performance of the FC. Polarization curves showed that the electrochemical reaction on both sides of the fuel cell is under the effect of mass transfer. Therefore the highest Open Circuit Potential (OCP) and

highest power density was recorded for counter current rather than cocurrent flow pattern at the same flow rates of hydrogen and air. On the other hand the polarization curves revealed that the values of the cell voltage, current density, and power density were inversely proportional with the increase of the hydrogen and air flow rates for both flow patterns (counter current and cocurrent) due to the increase in the rate of membrane dehydration as well as decreasing the rate of ion transfer. The lowest values of cell voltage, current density and power density in the polarization curves of counter-current flow were recorded when the flow rate of hydrogen was less than the flow rate of air. SEM images for the topography of the electrode surfaces and EDX analysis of the elements of the catalyst layer and Gas Diffusion Layer (GDL) before and after exposure to hydrogen and air gases showed an obvious degradation in the elements of the catalyst layer due to the galvanic corrosion phenomenon as a direct result of the electrochemical reaction among Pt–Ru (40%: 20% by wt.)/C which forms the catalyst layer in the anodic side and the hydrogen gas as well as the electrochemical reaction between the catalyst layer in the cathodic side and the water molecules formed due to the electrochemical reaction between H_2 and air. As a result of this assumption the metals in the combination might show an increase in the current to less negative values and other might show a decrease in the current to less positive values. In other words, the behavior of these metals in the given environment might respond in different manners so the more negative (active) metal in the combination might corrode sacrificially and get depleted to protect the other metals of less negativity (i.e. more noble). This act is also affected with the area of each metal in the couple as an important variable. As a result of the galvanic corrosion pits were formed in the catalyst layer. On the other hand the research team found that modified Nafion composite membrane containing SiO_2 produced in situ is better than the commercial membrane without SiO_2 in combating dehydration because the water uptake of the modified membrane is greater than the commercial membrane.

Acknowledgments

This work was supported by the Scientific Research Support Fund/Ministry of Higher Education and the Royal Scientific Society. Therefore the authors would like to thank the Scientific Research Support Fund/Ministry of Higher Education and the Royal Scientific Society for providing this support. The authors would like also to thank Eng. Hala F. Al Thnaibat, Eng. Nebal Alsaide, Eng. Abeer Dauood for assisting in the experimental work.

References

[1] Wu J, Yuan XZ, Martin JJ, Wang H, Shen J, Wu S, et al. A review of PEM fuel cell durability: degradation mechanisms and mitigation strategies. J Power Sources 2008;184(6):104–19.
[2] Sridhar P, Perumal R, Rajalakshmi N, Raja M, Dhathathreyan KS. Humidification studies on polymer electrolyte membrane fuel cel. J Power Sources 2001;101(1):72–8.
[3] Basu S. Recent Trends in Fuel Cell Science and Technology. 1st ed. Springer Publishing Co.; 2007.
[4] Buchi FN, Inaba M, Schmidt TJ. Polymer electrolyte fuel cell durability. 1st ed. Springer Publishing Co.; 2009.
[5] Zhang J. PEM fuel cell electrocatalysts and catalyst layers. 1st ed. Springer Publishing Co.; 2008.
[6] Basu S, Agarwal A, Pramanik H. Improvement in performance of a direct ethanol fuel cell: effect of sulfuric acid and Ni-mesh. Electrochem Commun 2008;10(6):1254–7.
[7] Chul M, Masayoshi I, Hiroshi I, Tetsuhiko M, Akihiro N, Yasuo H, et al. Influence of properties of gas diffusion layers on the performance of polymer electrolyte-based unitized reversible fuel cells. Int J Hydrogen Energy 2011;36(1):1740–53.
[8] Hongtan L, Andrew H. Effects of the difference in electrical resistance under the land and channel in a PEM fuel cell. Int J Hydrogen Energy 2011;36(1):1664–70.
[9] Kap-Seung C, Hyung-Man K, Sung-Mo M. Numerical studies on the geometrical characterization of serpentine flow-field for efficient PEMFC. Int J Hydrogen Energy 2011;36(1):1613–27.
[10] Luis V, Radu M, Marıá G, Jesuś M. Effect of the relative position of oxygen hydrogen plate channels and inlets on a PEMFC. Int. J. Hydrogen Energy 2010;36:11425–36.
[11] Santarelli MG, Torchio MF. Experimental analysis of the effects of the operating variables on the performance of a single PEMFC. J Energy Convers Manage 2007;48:40–51.
[12] Hsieh SS, Yang SH, Kuo JK, Huang CF, Tsai HH. Study of operational parameters on the performance of micro PEMFCs with different flow fields. J Energy Convers Manage 2006;47:1868–78.
[13] Miaomiao H, Gang Z, Mingyu L, Shuang W, Yang Z, Hongtao L, et al. Considerations of the morphology in the design of proton exchange membranes: cross-linked sulfonated polyetherether ketones using a new carboxyl-terminated benzimidazole as the cross-linker for PEMFCs. Int J Hydrogen Energy 2011;36:2197–206.
[14] Jin CS, Kan LH, Fanghei T. Performance of proton exchange membrane fuel cells at elevated temperature. J Energy Convers Manage 2011;52:3415–24.
[15] Afshari A, Jazayeri SA. Effect of the cell thermal behavior and water phase change on a proton exchange membrane fuel cell Performance. J Energy Convers Manage 2010;51:655–62.
[16] Tian J, Shi Z, Shi J, Shan Z. Preparation of water management layer and effects of its composition on performance of PEMFCs. J Energy Convers Manage 2008;49:1500–5.
[17] Alvarez A, Guzman C, Carbone A, Sacca A, Gatto I, Passalacqua E, et al. Influence of silica morphology in composite Nafion membranes properties. Int J Hydrogen Energy 2011;36:14725–33.
[18] Wang L, Liu H. Performance studies of PEM fuel cells with interdigitated flow fields. J Power Sources 2004;134:185–96.
[19] Dietmar G, Nada Z, Christian S, Florian G, Victor L, Christopher H. Effect of operating conditions on current density distribution and high frequency resistance in a segmented PEM fuel cell. Int J Hydrogen Energy 2012;37:7736–44.
[20] Sreenivasulu B, Vasu G, Dharma V, Naidu SV. Performance study of a PEM fuel cell with 4-Serpentine flow fields-experimental study. Int J f Eng Sci Adv Technol 2012;2:291–6.
[21] Park S, Shao Y, Viswanathan V, Liu J, Wang Y. Non-kinetic losses caused by electrochemical carbon in PEM fuel cells. Int J Hydrogen Energy 2012;37:8451–8.
[22] Fontana MG, Greene ND. Corrosion engineering. 3rd ed. McGraw-Hill; 1985.
[23] Uhlig HH. Corrosion and corrosion control. 3rd ed. John Wiely and Sons; 1985.
[24] Revie RW. Uhlig's corrosion handbook. 3rd ed. John Wiely and Sons; 2000.
[25] Bard AJ, Faulkner LR. Electrochemical methods: fundamentals and applications. 2nd ed. John Wiely and Sons; 2001.
[26] Mauritz KA, Moore RB. State of understanding of Nafion. Chem Rev 2004;104:4535–85.
[27] Gierke TD, Munn GE, Wilson FC. The morphology in Nafion perfluorinated membrane products, as determined by wide-angle and small-angle X-ray studies. J Polym Sci Part B: Polym Phys 1981;19:1687–704.